iScience

Article

The m6A reader HNRNPC is a key regulator in DSS-induced colitis by modulating macrophage phenotype

Graphical abstract

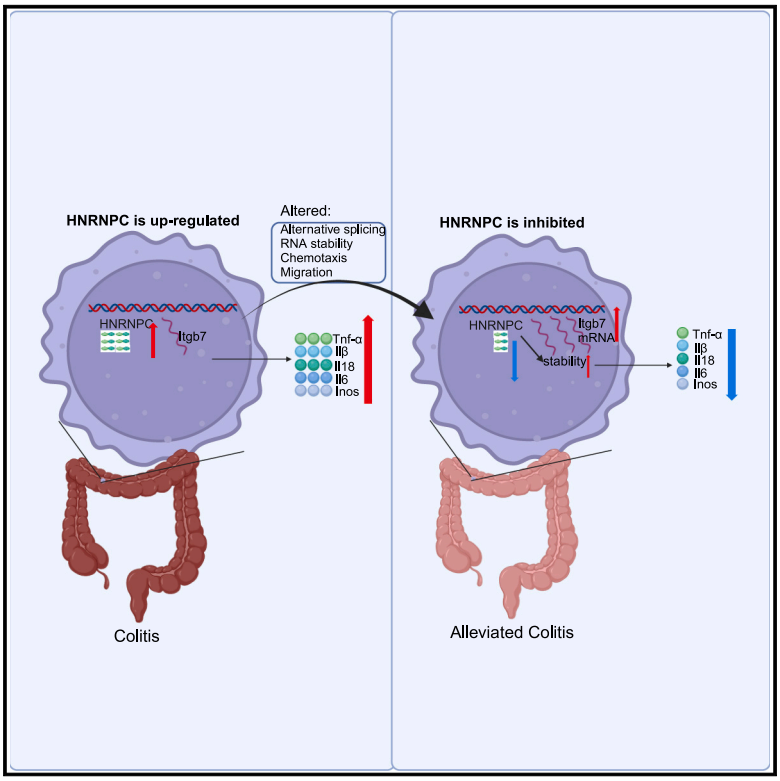

Highlights

- HNRNPC was upregulated in the colon macrophages in the DSS-induced colitis
- Inhibition of HNRNPC can mitigate macrophages' inflammation
- HNRNPC suppression in macrophages can alleviate colitis

Authors

Xiaohui Fang, Yu Zhang, Ziliang Ke, ..., Huiting Su, Jun Xu, Yulan Liu

Correspondence

xujun@hsc.pku.edu.cn (J.X.), liuyulan@pkuph.edu.cn (Y.L.)

In brief

Molecular biology; Immune response; Cell biology

Fang et al., 2025, iScience *28*, 111812
March 21, 2025
https://doi.org/10.1016/j.isci.2025.111812

CellPress

iScience

CellPress
OPEN ACCESS

Article

The m6A reader HNRNPC is a key regulator in DSS-induced colitis by modulating macrophage phenotype

Xiaohui Fang,[1,2] Yu Zhang,[1,2] Ziliang Ke,[1,2] Yang Zhang,[1,2] Yiken Lin,[1,2] Yibo Huang,[1,2] Jianhua Zhou,[3] Huiting Su,[3] Jun Xu,[1,2,*] and Yulan Liu[1,2,4,*]

[1]Department of Gastroenterology, Peking University Peoples Hospital, No.11, Xizhimen South Street, Xicheng District, Beijing 100044, China
[2]Clinical Center of Immune-Mediated Digestive Diseases, Peking University People's Hospital, No. 11, Xizhimen South Street, Xicheng District, Beijing 100044, China
[3]Institute of Clinical Molecular Biology & Central Laboratory, Peking University People's Hospital, Beijing 100044, China
[4]Lead contact
*Correspondence: xujun@hsc.pku.edu.cn (J.X.), liuyulan@pkuph.edu.cn (Y.L.)
https://doi.org/10.1016/j.isci.2025.111812

SUMMARY

m6A regulators were demonstrated to modulate the functions of intestinal epithelial and immune cells in the ulcerative colitis. This study aimed to elucidate whether and how the m6A reader heterogeneous nuclear ribonucleoprotein C (HNRNPC) regulates macrophage function in the colitis. We observed elevated HNRNPC in the inflammatory Raw264.7 cells and macrophages in the dextran sodium sulfate (DSS)-induced colitis. Knocking down HNRNPC can mitigate LPS-induced activation of macrophages *in vitro*. Furthermore, adoptive transfer of macrophages with HNRNPC knockdown significantly alleviated colitis compared to those transfected with negative control siRNA. Additionally, RNA sequencing illuminated that HNRNPC regulated functions of macrophages by inhibiting alternative mRNA slicing, involving adjusting acute inflammatory response, and promoting cell chemotaxis and migration. Besides, HNRNPC can govern the stability of Itgb7, and Itgb7 might be an effective target for HNRNPC in macrophages. Our findings highlight the crucial role and therapeutic potential of HNRNPC inhibition in macrophages in alleviating colitis.

INTRODUCTION

Inflammatory bowel disease (IBD) is a chronic and relapsing immunologically mediated inflammatory disease, including Crohn disease and ulcerative colitis (UC), whose etiology and pathogenesis are complicated and may involve intricate crosstalk among genetic factors, environmental effects, gut microbiota, and immune factors.[1–3] At present, IBD has developed into a global disease and brought tremendous burden to the worldwide healthcare system. Based on these, further investigation into the mechanisms behind IBD and potential therapies are necessary and meaningful.[4,5]

In recent years, mRNA post-transcriptional modification has become a new epigenetic regulation mechanism, among which N6-methyladenosine (m6A) methylation is the most abundant post-transcriptional modification of mRNA in mammals.[6,7] m6A is involved in the epigenetic regulation of multiple cellular processes and plays significant roles in influencing the stability, translation, and nuclear translocation of mRNA.[8,9] m6A is reversibly and dynamically regulated by three kinds of regulators. Simply, they are catalyzed through the m6A methyltransferases called "writers," removed by the demethylases called "erasers," and recognized by m6A-binding proteins called "readers."[10] Existing studies showed that the abnormal expression of m6A regulators can impact the development of multiple tumors by influencing immune cells, immune checkpoints, and other factors.[11,12] Additionally, the expression levels of m6A regulators fluctuate across various inflammatory diseases, and these regulators controlled the differentiation and phenotypic transformation of some cells to influence pathogenesis of inflammation, such as colitis.[13,14] m6A writer METTL3 controls T cell homeostasis and participates in regulating colitis[15]; m6A eraser ALKBH5 regulates the capacity of $CD4^+$ T cells to induce autoimmune colitis[16]; macrophages lacking m6A reader IGF2BP2 exhibited enhanced M1 phenotype and contributed to the progression of dextran sodium sulfate (DSS)-induced colitis.[14] These studies indicated that multiple m6A regulators took part in the pathogenesis of IBD.

Heterologous nuclear ribonucleoprotein C (HNRNPC) is an RNA-binding protein, binding to RNA transcripts and affecting the stability, splicing, transport, and translation of precursor mRNA. HNRNPC shows a stronger affinity for methylated RNA, and recognition of m6A by HNRNPC depends on RNA's structural changes.[17,18] HNRNPC's expression was altered in multiple tumors, contributing to tumor metastasis and invasion, which was linked to clinical poor prognosis.[19–21] At present, a few studies suggest the relationship between HNRNPC and inflammation or immune response. Jin et al.'s study found that silencing

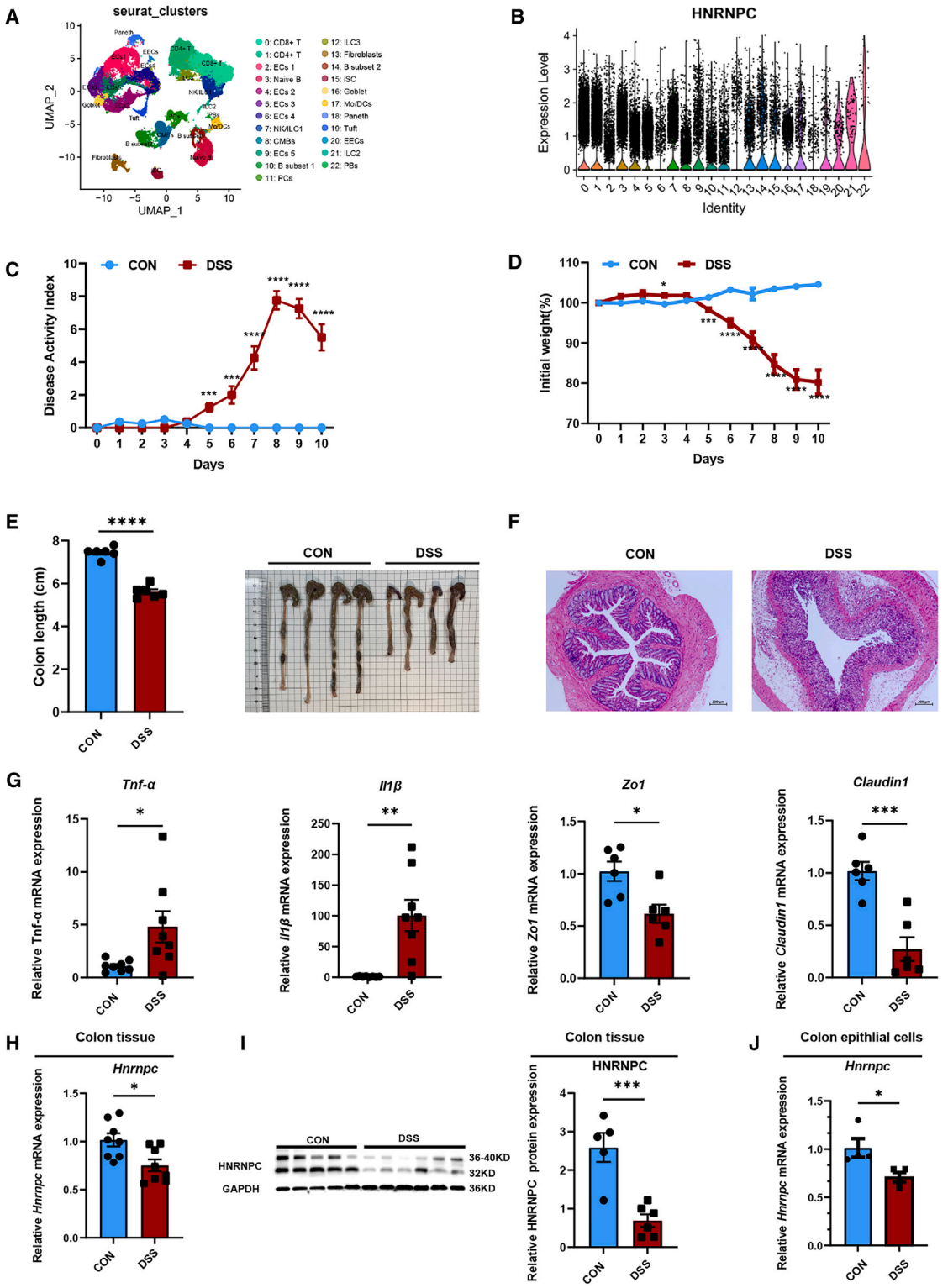

Figure 1. HNRNPC with broad expression across diverse colonic cells downregulates in DSS-induced colitis

Acute colitis was induced with 2.5% DSS (dextran sulfate sodium salt) in drinking water for 7 days and then with regular drinking water for another 3 days

(A) Twenty-three major clusters of colonic cells from three healthy controls and three patients with ulcerative colitis.

(B) Expression level of HNRNPC in 23 kinds of diverse colonic cells.

(C) Disease activity index during acute colitis.

(legend continued on next page)

HNRNPC can reduce the secretion of interferon alpha (IFN-α).[22] IFN-α, as a multi-effect cytokine, plays an important role in immune cell differentiation and activation, antigen presentation, and immune surveillance.[23] A previous study revealed that HNRNPC is broadly expressed across various cell types, with particularly high expression in M1 macrophages, GBM cancer cells, T cells, and natural killer (NK) cell in the glioblastoma microenvironment.[24] In addition, HNRNPC was considered to affect immune pathways and the infiltration of immune cells in the endometriosis.[25] Existing researches have indicated that HNRNPC plays a pivotal role in immune responses. Additionally, a host of researches supported that RNA-binding proteins can modulate inflammatory gene expression in macrophages, for example, the RNA-binding protein IGF2BP3 can mediate the polarization of macrophage toward an immunosuppressive phenotype.[26] The RNA-binding protein IGF2BP2 was reported to regulate macrophage phenotypic activation and inflammatory diseases.[14] hnRNP UL1, also as a binding protein, can prohibit NF-κB-triggered transcriptional expression of pro-inflammatory cytokines in response to innate stimuli in the macrophages.[27] And the RNA-binding proteins SRSF1 and HNRNPU can regulate MyD88 alternative splicing and LPS-induced cytokines' production in the macrophages.[28] Given the pivotal role of RNA-binding proteins in macrophages, we aim to investigate thoroughly whether HNRNPC can regulate macrophages' function.

Previous studies have demonstrated that macrophages are essential for maintaining intestinal homeostasis and regulating immune responses and tissue repair in the gut.[29] Macrophages play a critical role in both the inflammatory and repair phases of IBD. In the inflammatory phase of IBD, macrophages produce inflammatory cytokines upon activation by pathogen-associated molecular patterns (PAMPs), enhancing the immune response of Th1 and Th17 cells against invading microorganisms, thereby exacerbating epithelial damage. In the repair phase of IBD, macrophages promote epithelial cell proliferation and facilitate mucosal healing.[29–31] A comprehensive review about the heterogeneity of intestinal macrophages and their roles in intestinal health provides new insights for targeted therapies and stratified treatment approaches in patients with IBD.[32] These existing researches all suggested crucial role of macrophages in the pathogenesis and therapy of IBD. In addition, previous researches showed that m6A regulators controlled certain functions of macrophages, for instance, the m6A reader IGF2BP2 plays a role in regulating macrophage phenotypic activation.[14] However, the role of HNRNPC in macrophage remains unclear. Therefore, this study aimed to investigate the involvement of HNRNPC in macrophages during DSS-induced colitis.

In our current study, we used flow cytometry to determine the changes of HNRNPC in macrophages in the DSS-induced colitis. Then, the regulatory effect of HNRNPC on macrophages was evaluated in *in vitro* experiments, and transcriptome sequencing (RNA-Seq) was used to get a comprehensive understanding of how HNRNPC regulates these cells. Finally, the effect of HNRNPC knockdown in the macrophages on the DSS-induced colitis mice was evaluated by adoptive transfer of macrophages with HNRNPC knockdown. Our results emphasized the importance of inhibiting HNRNPC in macrophages to alleviate colitis.

RESULTS

HNRNPC is widely expressed across various types of intestinal cells

To identify m6A regulators with high expression levels in the intestine, we conducted single-cell sequencing on intestinal tissues obtained from three UC patients and three healthy individuals. Subsequently, cluster analysis was conducted on intestinal cells and 23 types of intestinal cell populations were identified (Figure 1A), including epithelial cells, Paneth cells, and various immune cells. Subsequently, we analyzed the expression of various m6A regulators in various intestinal cells (Figures S1A–S1C) and ultimately observed that HNRNPC was highly expressed in various intestinal cells (Figure 1B). These results provided a preliminary foundation for us to investigate the roles of different m6A regulators in IBD. And after comprehensive evaluation, we intended to explore the role of HNRNPC in DSS-induced colitis in our subsequent studies.

HNRNPC is downregulated in the DSS-induced colitis

We established a mouse model of acute dextran sulfate sodium colitis and evaluated the expression of HNRNPC. The acute colitis was characterized by ascending DAI score (Figure 1C), decreased body weight (Figure 1D), and shortened colon length (Figure 1E) of DSS mice. The H&E staining demonstrated a pronounced infiltration of inflammatory cells and extensive disruption of the mucosal structure and integrity (Figure 1F). The results obtained from qPCR indicated upregulation of *Tnf-α* and *Il1β*, as well as downregulation of *ZO1* and *Occludin* (Figure 1G). Following that, we conducted measurements on the expression level of the m6A reader HNRNPC in the colon tissue. The qPCR analysis revealed a downregulation in the expression of *Hnrnpc* (Figure 1H). The levels of HNRNPC protein displayed a consistent reduction (Figure 1I). Afterward, we isolated colonic epithelial cells and measured the mRNA level of HNRNPC, and the qPCR result indicated the decreased expression of *Hnrnpc* in

(D) The body weight percentage (relative to the initial weight, set as 100%) during the progression of acute DSS-induced colitis.
(E) Representative colonic images and colon length.
(F) Representative hematoxylin and eosin (H&E) images of the colon. Scale bar: 200 μm
(G) The relative mRNA expression of *Tnf-α*, *Il1β*, *Claudin1*, and *Zo1*.
(H) The relative mRNA expression of *Hnrnpc* in the colon tissue.
(I) The protein expression of HNRNPC in the colon tissues was determined by western blot.
(J) The relative mRNA expression of *Hnrnpc* in the epithelial cells. Data are represented as mean ± SEM. (n = 6–7/group). Two-sided Student's t test (E, G, H, I, and J) was performed. $^{*}p < 0.05$, $^{**}p < 0.01$, $^{***}p < 0.001$. CON, control group with normal water; DSS, colitis group with dextran sulfate sodium water; *Hnrnpc,* heterogeneous nuclear ribonucleoprotein C; *Tnfa*, tumor necrosis factor α; *Il1b*, interleukin-1β; *Zo1*, tight junction protein 1.

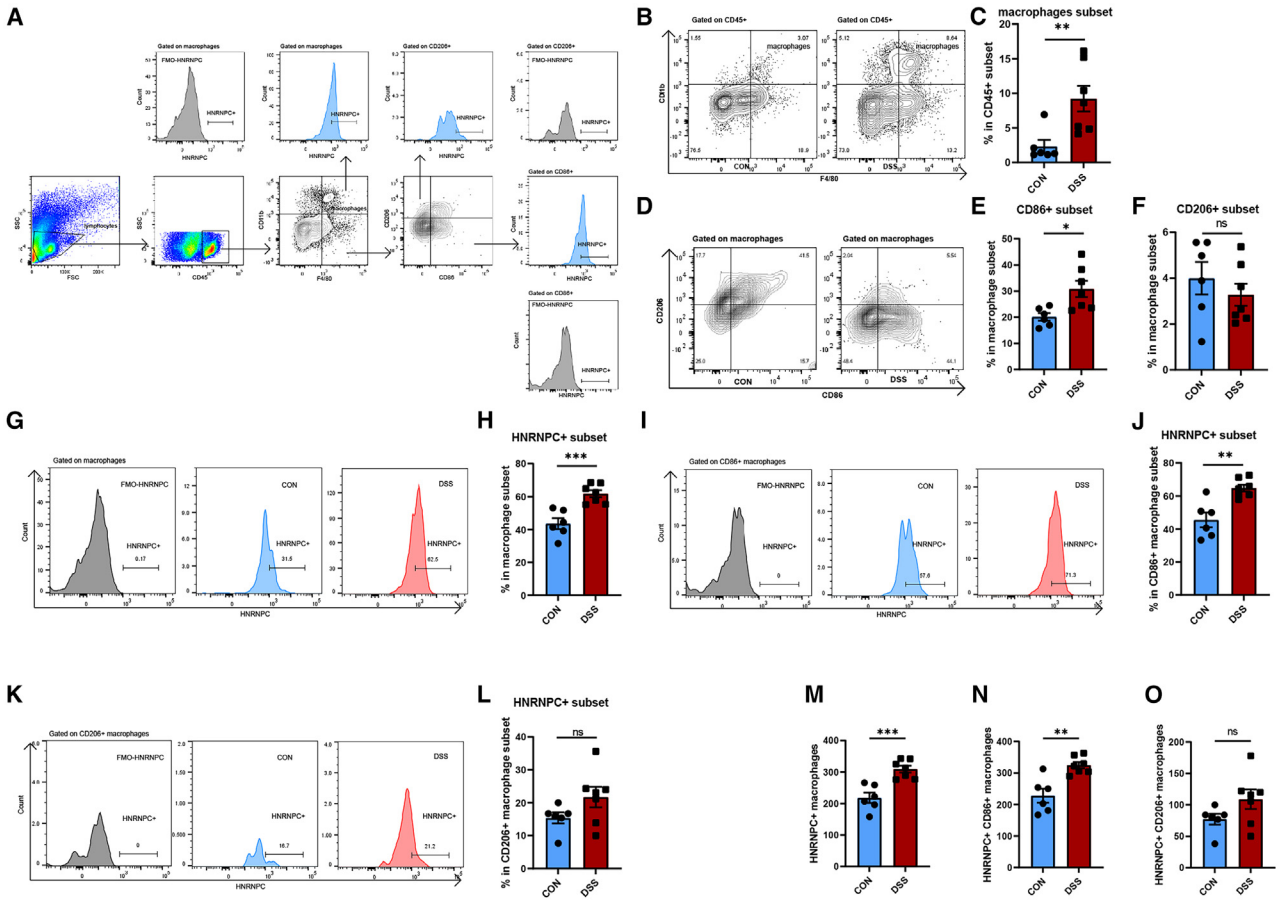

Figure 2. HNRNPC is upregulated in the macrophages of colonic lamina propria in the colitis

(A) Gate strategy of flow cytometry for analyzing the expression of HNRNPC in macrophages.

(B) Representative plots of ratio of the colonic CD45$^+$ F4/80$^+$ CD11b$^+$ macrophages in the CD45$^+$ lymphocytes and (D) quantitative analysis.

(C) Representative plots ratio of the colonic CD86$^+$ and CD206$^+$ macrophages and (E and F) quantitative analysis.

(G) Representative histograms of ratio of HNRNPC$^+$ in the colonic macrophages and (H) quantitative analysis.

(I) Representative histograms of ratio of HNRNPC$^+$ in the colonic CD86$^+$ macrophages and (J) quantitative analysis.

(K) Representative histograms of ratio of HNRNPC$^+$ in the colonic CD206$^+$ macrophages and (L) quantitative analysis.

(E and F) The cell number of HNRNPC+ macrophages, HNRNPC+ CD86$^+$ macrophages, and HNRNPC+ CD206+ macrophages (The total cell number of the three types of macrophages is 500). Data are represented as mean ± SEM. (n = 6–7/group). Two-sided Student's t test was performed. *$p < 0.05$, **$p < 0.01$, ***$p < 0.001$. ns: not significant. FMO, Fluorescence Minus One; CON, control group with normal water; DSS, colitis group with dextran sulfate sodium water.

the colitis group (Figure 1J). This indicated HNRNPC may participate in the occurrence and development of IBD. Additionally, we observed a significant decrease in the levels of *Mettl3*, *Fto*, *Alkbh5*, and *Ythdf1*, as well as elevated expression of *Mettl16*, *Ythdc1*, and *Hnrnpa2b1* in the colon tissue of mice treated with DSS (Figures S2A–S2C).

HNRNPC is upregulated in the macrophages of colonic lamina propria in the DSS-induced colitis

The expression of the same m6A modifier exhibits heterogeneity across distinct cellular populations. Therefore, we employed flow cytometry to further investigate the differential expression of HNRNPC across different immune cell types in the DSS-induced colitis. Initially, we assessed the changes in HNRNPC expression in macrophages (CD11b$^+$ F4/80$^+$). The identical gating strategy was employed to evaluate the expression of HNRNPC in macrophages, and FMO (Fluorescence Minus One) was utilized to precisely determine the localization of HNRNPC-positive cells (Figure 2A). Consistent with previous researches, the proportion of macrophages and CD86$^+$ macrophages in the colonic lamina propria of DSS-treated mice showed an increase (Figures 2B–2F). In the DSS-induced colitis group, the expression of HNRNPC in the macrophages was considerably enhanced, as depicted in Figures 2G and 2H when compared to the control group. In CD86$^+$ pro-inflammatory macrophages, the expression of HNRNPC was also markedly elevated (Figures 2I and 2J). Nevertheless, the CD206+ macrophages did not exhibit any noteworthy variation in HNRNPC levels (Figures 2K and 2L). And the cell numbers of HNRNPC+ macrophages and HNRNPC+ CD86$^+$ macrophages were more in the DSS group (Figures 2M and 2N), and number of HNRNPC+ CD206+ macrophages has no variation (Figure 2O).

In parallel, we employed flow cytometry to analyze the expression of HNRNPC in T and B lymphocytes. We continued to utilize the same gating strategy and FMO for HNRNPC (Figure S3A). In the DSS-induced colitis group, we did not observe significant expression changes of HNRNPC in B lymphocytes (Figures S3B and S3C), $CD4^+$ T cells (Figures S3D and S3E), and $CD8^+$ T cells (Figures S3F and S3G). Furthermore, we assessed the expression levels of HNRNPC in the innate lymphoid cells (ILCs) in the DSS group (Figure S4A). Our analysis revealed noticeable elevation in the expression of HNRNPC exclusively in ILC3 (Figures S4F and S4G). In contrast, no significant alterations in HNRNPC expression were observed in other ILC subsets, namely ILC1 and ILC2 (Figures S4B–S4E).

Considering the notable alterations of HNRNPC in macrophages as indicated by the aforementioned results, we conducted deeper researches to explore the function of HNRNPC in macrophages.

HNRNPC is upregulated in the Raw264.7 cells in the inflammatory condition

We employed the mouse macrophage cell line Raw264.7 to investigate the expression of HNRNPC in the macrophages under inflammatory conditions. After stimulating the cells with LPS (lipopolysaccharide) for 2 h, we observed an increasing trend in the expression of *Hnrnpc* and upregulation of various cytokines including *Tnf-α*, *Il1β*, *Il18*, *Inos*, and *Il6* (Figure 3A). Afterward, we treated cells with LPS for more hours. *Hnrnpc* displayed increased expression with LPS stimulation for 4, 6, 12, and 24 h (Figures 3B–3E). These findings aligned with the previous observation of elevated HNRNPC expression in macrophages derived from the model of DSS-induced colitis.

HNRNPC knockdown relives LPS-induced cellular inflammation *in vitro*

To investigate the function of HNRNPC in macrophages, we designed three pairs of small interfering RNA (siRNA) to specifically knock down HNRNPC in the Raw264.7 cells. Initially, we validated the knockdown efficiency of HNRNPC at the mRNA and protein levels (Figures 3F–3H). After analysis, siHNRNPC2 that most effectively downregulated HNRNPC expression at both the mRNA and protein levels was selected for subsequent experiments in our research. We initially successfully reduced the expression of HNRNPC in Raw264.7 cells using siRNA; following that, we stimulated cells with 1 μg/mL of LPS for different hours to induce inflammation. When stimulating cells for 2 h, *Il18* was downregulated in Raw264.7 cells treated with HNRNPC knockdown (Figure 3I). When treating cells with LPS for 4 h, we observed a decrease in tendency of *Tnf-α* in the siHNRNPC group (Figure 3J). After treating cells with LPS for 6 h, the expression of some cytokines such as *Il1β* and *Il6* decreased markedly, whereas *Tnf-α* and *Il18 tended to decline* in the siHNRNPC group (Figure 3K). Following LPS treatment for 12 h, the expression of Il1β significantly decreased, whereas *Tnf-α* and *Il6* exhibited a descending trend in the siHNRNPC group (Figure 3L). In the presence of LPS for 24 h, we observed a drop in the expression levels of cytokines such as *Tnf-α*, *Il1β*, *Il6*, *Inos*, and *Il18* upon knockdown of HNRNPC in Raw264.7 cells (Figure 3M), as compared to cells treated with non-specific control siRNA (siNC). Furthermore, we designed a piece of siRNA targeting HNRNPC to knock down HNRNPC in the THP-1 cells. As depicted in Figures 2N–P, HNRNPC was markedly downregulated at both the mRNA and protein levels. Following siRNA treatment, we stimulated THP-1 cells with 100 ng/mL and 500 ng/mL of LPS for different hours to induce inflammation. When treating cells for 4 h and at 100 ng/mL, *IL6* was downregulated in THP-1 cells treated with HNRNPC knockdown, and CCL8 tended to decrease (Figure 3Q). After treating cells with LPS for 24 h and at 100 ng/mL, the expression of *IL18*, *CCL2*, and *CCL8* decreased notably while IL-6 and CCL3 tended to decline in the siHNRNPC group (Figure 3R). In the presence of 500 ng/mL LPS for 24 h, we observed downregulated TNF-α, CCL2, and CCL3 upon knockdown of HNRNPC in the THP-1 cells with siHNRNPC (Figure 3S).

Adoptive transfer of macrophages with HNRNPC knockdown alleviates DSS-induced colitis

To further validate the role of HNRNPC knockdown in macrophages during DSS-induced colitis, we transferred HNRNPC-knockdown Raw264.7 cells into DSS-treated mice. On the day 0, 3, 5, and 7 of DSS-induced colitis, 2×10^6 cells were separately transferred to mice intravenously (Figure 4A). We found that mice receiving HNRNPC-knockdown macrophages (later called Raw-siHNRNPC mice) had mitigated colitis compared to those receiving macrophages transfected with siNC (later called Raw-siNC mice) as evidenced by decreased disease activity index (Figure 4B) and longer colon length (Figure 4D). H&E staining (Figure 4E) results indicated that Raw-siHNRNPC mice exhibited milder mucosal damage, more complete epithelial structure, and reduced inflammatory cell infiltration. We then employed flow cytometry to investigate the expression of HNRNPC in the colonic macrophages after transferring Raw264.7 cells with or without HNRNPC knockdown into DSS mice. We found there was downregulated HNRNPC in the macrophages in the Raw-siHNRNPC mice (Figures 4F–4H), which partly indicated the efficiency of silencing HNRNPC of Raw264.7 cells *in vivo*. We then measured the expression of some cytokines. The results showed that colon tissues in the Raw-siHNRNPC mice had increased anti-inflammatory cytokines characterized by slightly raised *Il10*, *Il4*, and *Il13* (Figure 4I), whereas expression of pro-inflammatory cytokines such as *Il6*, *Inos*, and *Il18* (Figure 4J) failed to change. In addition, we detected the expression of some tight junction proteins of colon tissue, and the levels of *Zo-1* and *Occludin* were increased (Figure 4K). It suggested that the inhibition of HNRNPC in macrophages could potentially confer a protective effect on the integrity of the intestinal epithelial barrier.

Downregulation of HNRNPC leads to alterations of inflammation, adhesion, and mRNA-splicing-related functions in the macrophages

To illuminate potential mechanisms by which HNRNPC regulates macrophages, we performed transcriptome analysis on mouse macrophage cell line Raw264.7 cells with and without HNRNPC knockdown. And we found numerous downregulated and upregulated differentially expressed genes (DEGs) in the macrophages with HNRNPC knockdown as compared to control macrophages (Figure 5A). Among these genes,

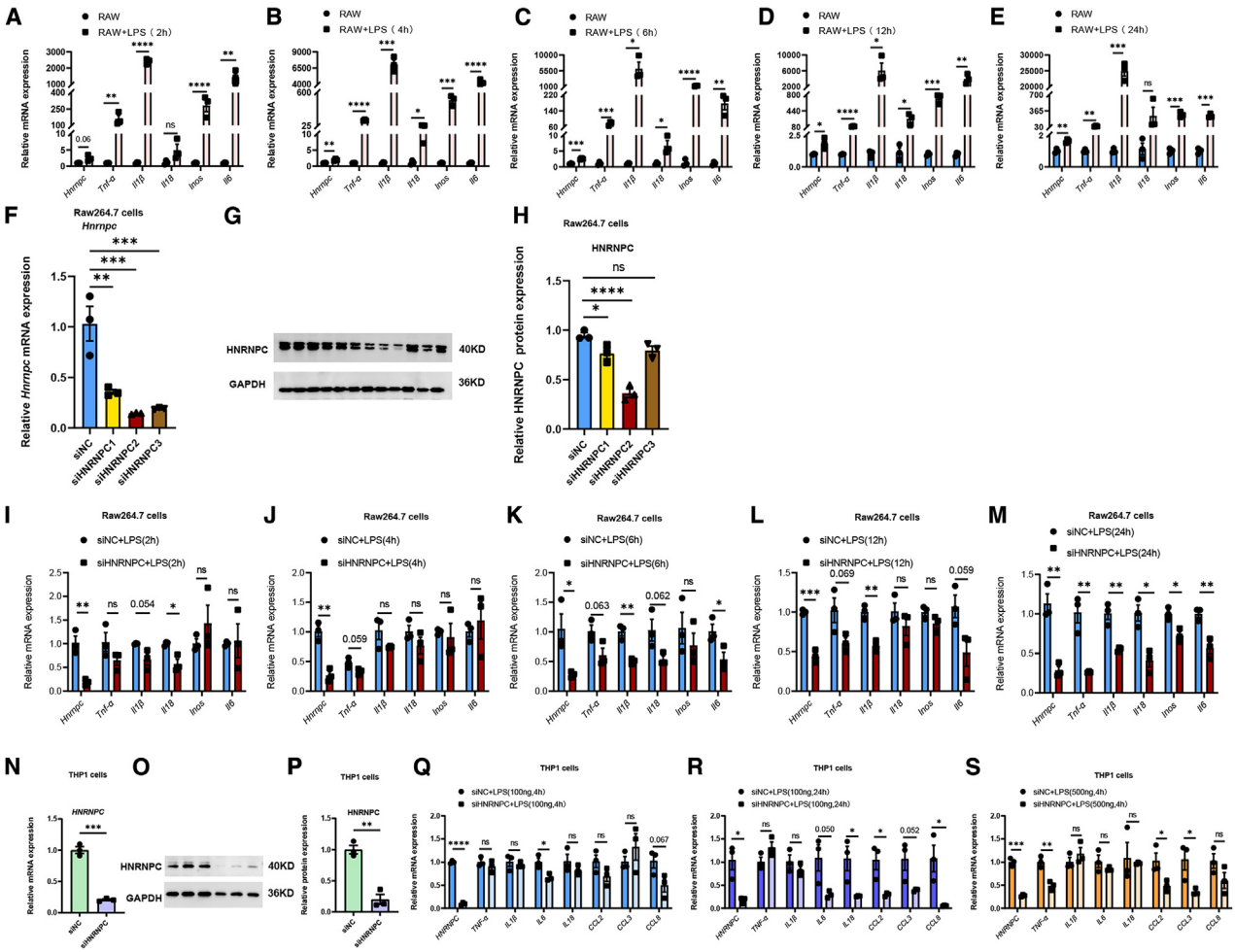

Figure 3. HNRNPC knockdown relives LPS-induced cellular inflammation in vitro

(A–E) The relative mRNA expression of *Hnrnpc, Tnf-α*, *Il1β*, *Il18*, *Inos*, and *Il6* after 2, 4, 6, 12, and 24 h treatment with LPS in the Raw264.7 cells.

(F) The relative mRNA expression of *Hnrnpc* after transfected with siHNRNPC-1,2,3, or negative control for 24 h in the Raw264.7 cells.

(G, H) The relative protein expression of HNRNPC after transfected with siHNRNPC-1,2,3 or negative control for 48 h in the Raw264.7 cells was determined by western blot.

(I–M) The relative mRNA expression of *Hnrnpc, Tnf-α*, *Il1β*, *Il18, Inos*, and *Il6* in the siNC + LPS and siHNRNPC + LPS groups. (After Raw264.7 cells are transfected with siRNA for 24h, LPS was added to treat the cells for another 2, 4, 6, 12, and 24 h).

(N) The relative mRNA expression of *HNRNPC* after transfected with siHNRNPC or negative control for 24h in the THP1 cells.

(O, P) The relative protein expression of HNRNPC after transfected with siHNRNPC or negative control for 48 h in the THP1 cells was determined by western blot.

(Q–S) The relative mRNA expression of HNRNPC, TNF-α, IL1β, IL6, Il18, CCL2, CCL3, and CCL8 in the siNC + LPS and siHNRNPC + LPS groups. (After THP1 cells are transfected with siRNA for 24 h, 100 ng/mL or 500 ng/mL LPS was added to treat the cells for another 4 or 24 h). Data represent three independent experiments and are represented as mean ± SEM. (*n* = 3/group). Two-sided Student's t test (A–E and I–M) was performed. One-way ANOVA was applied in Figures 5F and 5H. $^{*}p < 0.05$, $^{**}p < 0.01$, $^{***}p < 0.001$, $^{****}p < 0.0001$. ns: not significant. Raw, Raw264.7 cells group without additional treatment; Raw+LPS, Raw264.7 cells after LPS treatment; siNC, Raw264.7, or THP1 cells with negative control siRNA treatment; siHNRNPC, Raw264.7, or THP1 cells with siHNRNPC treatment; siNC/siHNRNPC + LPS, Raw264.7, or THP1 cells with siRNA and LPS; LPS, lipopolysaccharide; *Hnrnpc*, heterogeneous nuclear ribonucleoprotein C; *Tnf-α*, tumor necrosis factor alpha; Il, interleukin; *Inos*, inducible nitric oxide synthase; CCL, C-C motif chemokine ligand 2.

Odc1 can suppress the inflammatory response of macrophages and prevent cell apoptosis induced by ROS,[33] and *Tnfrsf9* (also called *Cd137*) was found to induce macrophages apoptosis.[34] Gene Ontology (GO) enrichment analysis confirmed that knocking down HNRNPC led to alterations in components associated with macrophage cell adhesion, cell migration, and chemotaxis, as well as variations in defense responses against bacteria (Figure 5B). Furthermore, the analysis of gene set enrichment analysis (GSEA) indicated that the knockdown of HNRNPC resulted in the inhibition of cellular functions related to mRNA splicing, processing, metabolism, and binding; meanwhile, the defense response against bacteria was activated (Figure 5C). As an m6A reader, HNRNPC mainly affects the stability, splicing, nuclear export, and translation of precursor mRNA. These results rightly conformed to the function of HNRNPC as a reader.[17]

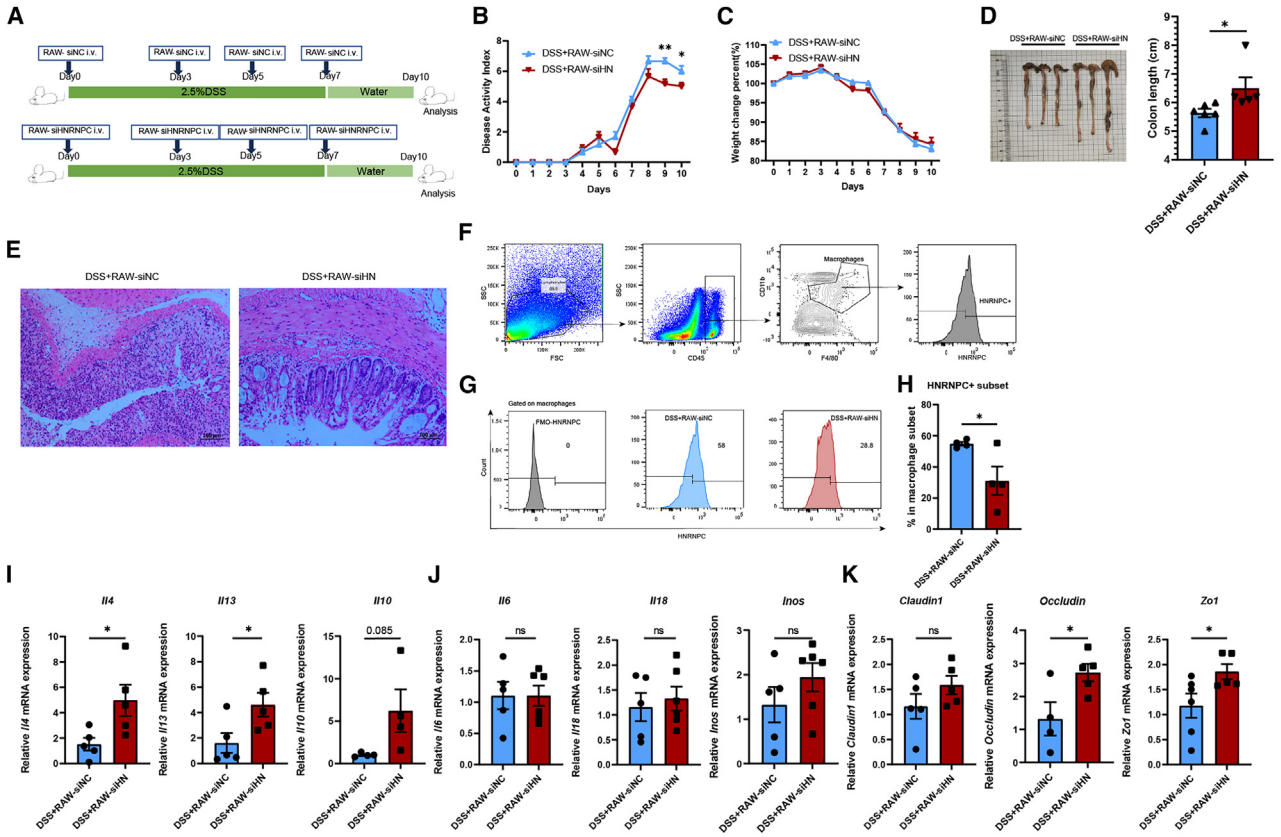

Figure 4. Adoptive transfer of macrophages with HNRNPC knockdown alleviates DSS-induced colitis

(A) Schematic diagram displaying the comprehensive design. Mice were treated with drinking water containing 2.5% DSS. On the day 0, 3, 5, and 7 of DSS-induced colitis, 2*10^6 cells were separately transferred to mice intravenously.

(B) Disease activity index during acute colitis.

(C) The body weight percentage (relative to the initial weight, set as 100%) during the progression of acute DSS-induced colitis.

(D) Representative colonic images and colon length.

(E) Representative hematoxylin and eosin (H&E) images of the colon. Scale bar: 100 μm

(F) Gate strategy of flow cytometry for analyzing the expression of HNRNPC in macrophages in the colonic lamina propria.

(G) Representative histograms of ratio of HNRNPC^{+} in the colonic macrophages and (H) quantitative analysis.

(I) The relative mRNA expression of anti-inflammatory cytokines including *Il4*, *Il13*, and *Il10*.

(J) The relative mRNA expression of pro-inflammatory cytokines including *Il6*, *Il18*, and *Inos*.

(K) The relative mRNA expression of intestinal epithelial barrier makers including *Zo1*, *Occludin*, and *Claudin1*. Data are represented as mean ± SEM. (n = 5–6/group). Two-sided Student's t test was performed. *$p < 0.05$, ns: not significant. DSS+Raw-siNC, mice subjected to induction of colitis and the transfer of Raw264.7 cells transfected with negative control siRNA; DSS+Raw-siHN, mice subjected to induction of colitis and the transfer of Raw264.7 cells with HNRNPC knockdown; *Il*, interleukin; *Inos*, inducible nitric oxide synthase; *Zo1*, tight junction protein 1.

Besides, GSEA enrichment plot revealed that pathways associated with alternative RNA splicing (Figure 5D), and RNA recognition (Figures S5A, S5C, and S5E) and binding (Figure S5M) and RNA export from nucleus (Figures S5K and S5L) were inhibited. And related DEGs include genes encoding m6A regulators (*Ythdc1*, *Hnrnpa2b1*, and *Rbm15*) (Figures 5D, S5B, S5D, and S5F). And the pathway pertaining to acute inflammatory response to antigenic stimulus was activated, and corresponding DEGs include H2−Q1 *Serpinb9*, H2−Q6, H2−Q4, and H2−D1 (Figure 5E). Additionally, GSEA enrichment plot showed stimulated pathways such as cell chemotaxis, adhesion, and migration (Figures 5F, S5G, S5I, S5N, and S5O) and correlated DEGs include *Ccl6*, *Ccl22*, *Cxcl16*, *Cd11c*, *Itgb7*, and *Spp1* (Figures 5F, S5H, and S5J).

qPCR analysis verified that HNRNPC knockdown significantly upregulated the expression of *Odc1*, *Anxa1*, and *Igtb7* (Figure 5G) while downregulated the expression of *Cd33* (Figure 5H) in the macrophages. However, no significant difference was observed in the mRNA expression of *Cd137*, *Wtap*, *Hnrnpa2b1*, *Cd11c*, *Spp1*, *Ccl22*, and *Cxcl16* (Figure 5I). The findings indicate that HNRNPC potentially exerts a substantial influence on macrophage function, specifically in relation to inflammation, adhesion, and mRNA splicing processes within the macrophages.

HNRNPC downregulation facilitates *Itbg7* expression by improving its stability

The aforementioned results indicated that *Odc1*, *Anxa1*, *Igtb7*, and *Cd33* may serve as possible targets of HNRNPC.

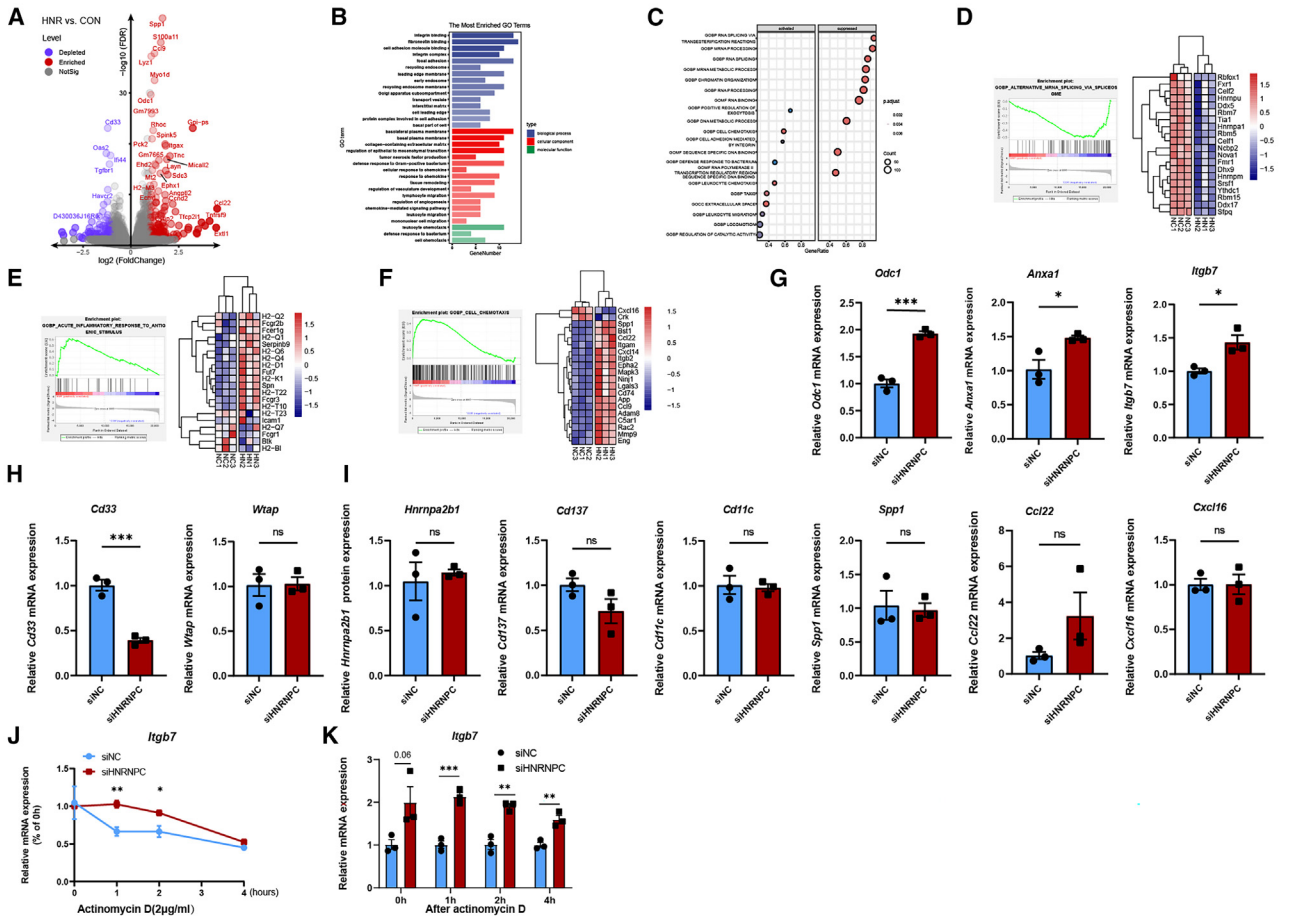

Figure 5. Downregulation of HNRNPC leads to alterations of inflammation, adhesion, and mRNA-splicing-related functions

(A) A volcano plot was generated using RNA-seq data to compare HNRNPC knockeddown (KD) and wild-type (WT) Raw264.7 cells. The x axis displays the log2 fold changes (FC), and the y axis represents the −log10 *p* value for HNRNPC KD compared to HNRNPC WT. Downregulated genes are depicted as blue dots, and upregulated genes are shown as red dots.

(B) GO enrichment analysis containing biological process, cellular component, and molecular function for HNRNPC knockdown.

(C) GSEA dot plot containing activated and suppressed pathways.

(D–F) Representative signaling pathways and their associated genes in the Raw264.7 cells with HNRNPC knockdown from GSEA analysis.

(G–I) qPCR was used to verify the differentially expressed genes in the Raw264.7 cells with or without HNNRPC knockdown. (*n* = 3/group).

(J) The relative level of *Itgb7* mRNA was examined by qPCR in Raw264.7 cells after HNRNPC knockdown and actinomycin D treatment (2 μg/mL) for 1, 2, and 4 h. The mRNAs at various time points were normalized to the t = 0 level (100%).

(K) The relative mRNA level of *Itgb7* in the siNC and siHNRNPC groups at various time points of actinomycin D treatment. Data are represented as mean ± SEM, and two-sided Student's t test was performed. GSEA, gene set enrichment analysis; GO, Gene Ontology. siNC, Raw264.7 cells with negative control siRNA treatment; siHNRNPC, Raw264.7 cells with siHNRNPC treatment.

Considering that HNRNPC can regulate mRNA stability,[35] we employed an RNA synthesis inhibitor actinomycin D to block new mRNA generation to verify whether HNRNPC can modulate stability of these target genes. We detected that after treated with actinomycin D, *Igtb7* degraded slower in macrophages with HNRNPC knockdown than macrophages treated with siNC (Figure 5J). In addition, we analyzed the expression of *Igtb7* at different time point of actinomycin D treatment in the macrophages with and without HNRNPC knockdown. We discovered that regardless of the duration of actinomycin D stimulation, the expression of *Igtb7* consistently rose whenever HNRNPC was suppressed (Figure 5K). These results are consistent with both our RNA-seq and qPCR data. We also detected the decay of *Odc1*, *Anxa1*, and *Cd33* after actinomycin D treatment, and we did not observe the influence of HNRNPC on the stability of *Odc1* and *Anxa1* (data were not shown). Interestingly, the decay of *Cd33* mRNA became slower (Figure S6A), but the expression of *Cd33* consistently decreased when HNRNPC was inhibited under actinomycin D stimulation (Figure S6B), which implied that HNRNPC did not regulate *Cd33* by affecting its stability, and deeper researches were required to elucidate the mechanism.

DISCUSSION

Our current research has revealed a notable increase in the expression of HNRNPC in macrophages during DSS-induced colitis. *In vitro* studies have revealed the role of HNRNPC in modulating the secretion of inflammatory cytokines in macrophages. Compared with transferring macrophages treated with siNC, transferring macrophages with HNRNPC knockdown into mice can alleviate DSS-induced colitis. Our transcriptome sequencing findings demonstrated that HNRNPC exerts regulatory effect over macrophage function through its influence on mRNA splicing, processing, metabolism, and binding activities. We discovered that m6A reader HNRNPC may regulate macrophage function by affecting the stability of *Itgb7*.

Previous studies on m6A have mostly focused on various tumors, and alterations in RNA m6A modification resulted in tumor progression and metastasis by affecting related transcripts and their associated functional pathways.[36] However, in recent years, significant functions of m6A in IBD have gradually been unveiled. Specifically, several m6A regulators played a significant role in colitis by influencing functions of epithelial cells or immune cells in the intestine. For instance, m6A eraser FTO downregulation led to increased S1P accumulation in IECs, thereby exacerbating colitis through m6A-dependent mechanisms. Lower FTO expression may cause UC patients to respond to vedolizumab treatment better.[37] And another study showed that depletion of METTL14 induced the development of spontaneous colitis.[38] In addition, alterations of m6A regulators in immune cells may also exert an influence on the intestine, leading to diverse changes of intestinal inflammation. In the classic study on m6A methylation controlling T cell homeostasis, METTL3 deficiency of T cells failed to undergo homeostasis expansion and remained significantly in their naive state, thereby preventing the occurrence of colitis.[15] Previous research found that mice with T cells lacking m6A writer WTAP developed colitis at a young age.[39] And another research discovered that an m6A eraser, ALKBH5, controlled CD4+ T cell ability to induce autoimmune colitis.[16] And our study proved the ability of HNRNPC, as an m6A reader, controlled the function of macrophages, thereby participating in development of DSS-induced colitis.

In our research, we found HNRNPC was also upregulated in colonic ILC3 cells in the DSS-induced colitis. ILC3 cells are involved in gastrointestinal immune responses, protecting the intestinal mucosa from infections by pathogens, thus maintaining intestinal homeostasis in the steady state; yet in pathological conditions, ILC3 exacerbates the progression of IBD.[40] Additionally, ILC3 cells interact with macrophages to collaboratively sustain intestinal homeostasis.[41] Therefore, investigating how HNRNPC regulates ILC3 would also be valuable; however, given that there was certain existing research basis on m6A in macrophages from other researches, our study initially focused on HNRNPC and macrophages. And in future, we will proceed to study whether and how HNRNPC modulates the function of ILC3 cells.

As previously described, HNRNPC has been implicated to promote invasion and metastasis in tumors. As an RNA-binding protein, HNRNPC regulates alternative splicing of targeting protein in a m6A-dependent manner. In research related with pancreatic ductal adenocarcinoma (PDAC), HNRNPC facilitated the progression of PDAC by controlling the alternative splicing of TAF8.[42] Another study proved that ALKBH5 downregulated the m6A modification of DDX58 mRNA, which caused HNRNPC bound to less m6A site of DDX58 mRNA, thereby inhibiting maturation of DDX58.[22] And our RNA-seq results also indicated that when HNRNPC was knocked down, several splicing-related functions and pre-mRNA binding were suppressed. In addition, downregulation of HNRNPC could suppress the stability of HIF1A mRNA, thereby reducing HIF1A expression and inhibiting the metastasis of hepatocellular carcinoma.[35] In our study, after HNRNPC was inhibited, some molecules related with inflammatory response also got lower expression; for example, *Cd33*, as a Siglec, could induce pro-inflammatory cytokine secretion and inhibit IFN-α production and cell adhesion.[43] And our results found that expression of *Cd33* was markedly downregulated when HNRNPC in macrophages was knocked down. However, when treated with actinomycin D, the stability of *Cd33* did not get inhibited accordingly when HNRNPC was knocked down. This manifested that *Cd33* was not direct target of HNRNPC or HNRNPC may regulate *Cd33* in other possible ways. But surprisingly, we discovered that HNRNPC downregulation raised *Itbg7* expression by improving its stability, which suggested that *Itbg7* can serve as the target of HNRNPC. As our RNA-seq data showed, Itgb7 was associated with chemotaxis and migration, and a previous study clarified that *Itbg7* controlled enterocyte migration in the small intestine.[44] The mentioned results hinted that HNRNPC might influence the chemotaxis and migration of macrophages by modulating Itgb7, and further studies were needed to verify this hypothesis.

In our current study, we found expression of HNRNPC in the colon tissue was downregulated in DSS-induced colitis, and its expression in the epithelial cells was also decreased. However, its expression was increased in the macrophages. There were some possible reasons as follows. First, m6A modification was widely present in various cells and regulated dynamically by m6A regulators.[45] Furthermore, the identical m6A modification can demonstrate diverse functions among different cellular types. For example, deletion of METTL3 in mouse T cells disrupted T cell homeostasis and differentiation and prevented colitis in a lymphogenic mouse adoptive transfer model.[15] However, in another research, overexpression of METTL3 aggravated LPS-induced intestinal epithelial inflammation and DSS-induced colitis.[46] Similarly, IGF2BP1 ablation in the intestinal epithelial caused destructed barrier function and aggravated DSS-induced colitis.[47] However, IGF2BP1 silencing markedly inhibited LPS-induced production of multiple pro-inflammatory cytokines in macrophages.[48] In accordance with IGF2BP1, our current study also verified that HNRNPC had a similar function in the macrophages. And roles of HNRNPC in intestinal epithelial in DSS-induced colitis were still worthy of further investigation.

In conclusion, our study proved that m6A regulator HNNRPC could modulate the production of pro-inflammatory cytokines of macrophages and that macrophages with HNRNPC-silencing can improve DSS-induced colitis. The functional regulation of macrophages by HNRNPC encompasses alternative splicing and maturation of precursor mRNA, as well as involvement in inflammatory response, adhesion, and chemotaxis. Itgb7 may

serve as a promising target for HNRNPC in macrophages. The findings indicate that regulating HNRNPC in macrophages could have therapeutic potential in the improvement of IBD.

Limitations of the study

Our research proved significant role of m6A reader HNRNPC in regulating macrophages in the DSS-induced colitis; however, there are several limitations that should be considered. Firstly, we transferred Raw264.7 cells transfected with siRNA into mice to prove the regulation of HNRNPC on macrophages in the colitis, but employing conditional knockout mice may better verify this effect if possible. In addition, we found HNRNPC can regulate Itbg7 by altering its stability, but whether and how Itgb7 influences macrophage's function needs deeper investigation. Besides, in this study, we only used male C57BL/6 J wild-type mice aged 6–8 weeks as research subjects but ignored the possible effects of gender on the study.

RESOURCE AVAILABILITY

Lead contact

Further information and requests for resources and reagents should be directed to and will be fulfilled by the lead contact, Prof. Yulan Liu (liuyulan@pkuph.edu.cn).

Materials availability

This study did not generate new unique reagents.

Data and code availability

- Single-cell sequencing and RNA-seq data have been deposited at the public database https://ngdc.cncb.ac.cn and are publicly available. Accession numbers are listed in the key resources table. Microscopy data reported in this paper will be shared by the lead contact upon request.
- This paper does not report original code.
- Any additional information required to reanalyze the data reported in this paper is available from the lead contact upon request.

ACKNOWLEDGMENTS

This work was supported by the National Natural Science Foundation of China (No. 82370555 to X.J., No. 82370537, and No. 82341228 to L.Y.L.), the Capital Health Research and Development of Special (No. CFH2024-1-4081 to L.Y.L. and No. CFH2024-4-4089 to X.J.), the Beijing Municipal Natural Science Foundation (No. 7232196 to L.Y.L.), and Peking University People's Hospital Scientific Research Development Funds (No. RDJP2023-22 to X.J.). We express our gratitude to the staff of the Institute of Clinical Molecular Biology & Central Laboratory at Peking University People's Hospital for their valuable technical support. We also acknowledge *BioRender.com* for providing a platform for us to design the graphical abstract.

AUTHOR CONTRIBUTIONS

Y. Liu and J.X. designed the study. X.F. reviewed the literature, performed the experiments, and analyzed the data. Yu Zhang, Z.K., Yang Zhang, Y. Lin, Y.H., J.Z., and H.S. helped in the execution of the mouse experiments. J.X performed the transcriptomic analysis and single-cell RNA sequencing data analysis. X.F. wrote the paper. J.X. and Y. Liu helped improving the manuscript and providing supervision for the project.

DECLARATION OF INTERESTS

The authors declare no competing interests.

STAR★METHODS

Detailed methods are provided in the online version of this paper and include the following:

- KEY RESOURCES TABLE
- EXPERIMENTAL MODEL AND STUDY PARTICIPANT DETAILS
  - Ethics approval and experimental animals
- METHOD DETAILS
  - Induction of acute dextran sulfate sodium colitis mouse model
  - Hematoxylin and eosin (H&E) staining
  - RNA extraction and quantitative real-time PCR (qPCR)
  - Western blot
  - Isolation of colon lymphocytes from the lamina propria
  - Isolation of colon epithelial cells
  - *Flow cytometry* analysis
  - Cell culture
  - siRNA knockdown
  - Adoptive transfer of Raw264.7 cells into mice with DSS-induced colitis
  - Single-cell RNA sequencing (scRNA-Seq) and bioinformatic analysis
  - Bulk RNA sequencing (RNA-Seq) and bioinformatic analysis
  - RNA stability assay
- QUANTIFICATION AND STATISTICAL ANALYSIS

SUPPLEMENTAL INFORMATION

Supplemental information can be found online at https://doi.org/10.1016/j.isci.2025.111812.

Received: April 6, 2024
Revised: July 25, 2024
Accepted: January 10, 2025
Published: January 16, 2025

REFERENCES

1. Ahluwalia, B., Moraes, L., Magnusson, M.K., and Öhman, L. (2018). Immunopathogenesis of inflammatory bowel disease and mechanisms of biological therapies. Scand. J. Gastroenterol. *53*, 379–389. https://doi.org/10.1080/00365521.2018.1447597.
2. Ananthakrishnan, A.N. (2015). Epidemiology and risk factors for IBD. Nat. Rev. Gastroenterol. Hepatol. *12*, 205–217. https://doi.org/10.1038/nrgastro.2015.34.
3. Schirmer, M., Garner, A., Vlamakis, H., and Xavier, R.J. (2019). Microbial genes and pathways in inflammatory bowel disease. Nat. Rev. Microbiol. *17*, 497–511. https://doi.org/10.1038/s41579-019-0213-6.
4. Kaplan, G.G. (2015). The global burden of IBD: from 2015 to 2025. Nat. Rev. Gastroenterol. Hepatol. *12*, 720–727. https://doi.org/10.1038/nrgastro.2015.150.
5. Ng, S.C., Shi, H.Y., Hamidi, N., Underwood, F.E., Tang, W., Benchimol, E.I., Panaccione, R., Ghosh, S., Wu, J.C.Y., Chan, F.K.L., et al. (2017). Worldwide incidence and prevalence of inflammatory bowel disease in the 21st century: a systematic review of population-based studies. Lancet *390*, 2769–2778. https://doi.org/10.1016/s0140-6736(17)32448-0.
6. Dorn, L.E., Lasman, L., Chen, J., Xu, X., Hund, T.J., Medvedovic, M., Hanna, J.H., van Berlo, J.H., and Accornero, F. (2019). The N(6)-Methyladenosine mRNA Methylase METTL3 Controls Cardiac Homeostasis and Hypertrophy. Circulation *139*, 533–545. https://doi.org/10.1161/circulationaha.118.036146.
7. Uddin, M.B., Wang, Z., and Yang, C. (2021). The m(6)A RNA methylation regulates oncogenic signaling pathways driving cell malignant

transformation and carcinogenesis. Mol. Cancer *20*, 61. https://doi.org/10.1186/s12943-021-01356-0.

8. Wang, H., Hu, X., Huang, M., Liu, J., Gu, Y., Ma, L., Zhou, Q., and Cao, X. (2019). Mettl3-mediated mRNA m(6)A methylation promotes dendritic cell activation. Nat. Commun. *10*, 1898. https://doi.org/10.1038/s41467-019-09903-6.
9. Ma, Z., Gao, X., Shuai, Y., Xing, X., and Ji, J. (2021). The m6A epitranscriptome opens a new charter in immune system logic. Epigenetics *16*, 819–837. https://doi.org/10.1080/15592294.2020.1827722.
10. Vu, L.P., Cheng, Y., and Kharas, M.G. (2019). The Biology of m(6)A RNA Methylation in Normal and Malignant Hematopoiesis. Cancer Discov. *9*, 25–33. https://doi.org/10.1158/2159-8290.Cd-18-0959.
11. Wan, W., Ao, X., Chen, Q., Yu, Y., Ao, L., Xing, W., Guo, W., Wu, X., Pu, C., Hu, X., et al. (2022). METTL3/IGF2BP3 axis inhibits tumor immune surveillance by upregulating N(6)-methyladenosine modification of PD-L1 mRNA in breast cancer. Mol. Cancer *21*, 60. https://doi.org/10.1186/s12943-021-01447-y.
12. Han, D., Liu, J., Chen, C., Dong, L., Liu, Y., Chang, R., Huang, X., Liu, Y., Wang, J., Dougherty, U., et al. (2019). Anti-tumour immunity controlled through mRNA m(6)A methylation and YTHDF1 in dendritic cells. Nature *566*, 270–274. https://doi.org/10.1038/s41586-019-0916-x.
13. Chen, X., Gong, W., Shao, X., Shi, T., Zhang, L., Dong, J., Shi, Y., Shen, S., Qin, J., Jiang, Q., and Guo, B. (2022). METTL3-mediated m(6)A modification of ATG7 regulates autophagy-GATA4 axis to promote cellular senescence and osteoarthritis progression. Ann. Rheum. Dis. *81*, 87–99. https://doi.org/10.1136/annrheumdis-2021-221091.
14. Wang, X., Ji, Y., Feng, P., Liu, R., Li, G., Zheng, J., Xue, Y., Wei, Y., Ji, C., Chen, D., and Li, J. (2021). The m6A Reader IGF2BP2 Regulates Macrophage Phenotypic Activation and Inflammatory Diseases by Stabilizing TSC1 and PPARγ. Adv. Sci. *8*, 2100209. https://doi.org/10.1002/advs.202100209.
15. Li, H.B., Tong, J., Zhu, S., Batista, P.J., Duffy, E.E., Zhao, J., Bailis, W., Cao, G., Kroehling, L., Chen, Y., et al. (2017). m(6)A mRNA methylation controls T cell homeostasis by targeting the IL-7/STAT5/SOCS pathways. Nature *548*, 338–342. https://doi.org/10.1038/nature23450.
16. Zhou, J., Zhang, X., Hu, J., Qu, R., Yu, Z., Xu, H., Chen, H., Yan, L., Ding, C., Zou, Q., et al. (2021). m(6)A demethylase ALKBH5 controls CD4(+) T cell pathogenicity and promotes autoimmunity. Sci. Adv. *7*, eabg0470. https://doi.org/10.1126/sciadv.abg0470.
17. Liu, N., Dai, Q., Zheng, G., He, C., Parisien, M., and Pan, T. (2015). N(6)-methyladenosine-dependent RNA structural switches regulate RNA-protein interactions. Nature *518*, 560–564. https://doi.org/10.1038/nature14234.
18. Zhou, K.I., Parisien, M., Dai, Q., Liu, N., Diatchenko, L., Sachleben, J.R., and Pan, T. (2016). N(6)-Methyladenosine Modification in a Long Noncoding RNA Hairpin Predisposes Its Conformation to Protein Binding. J. Mol. Biol. *428*, 822–833. https://doi.org/10.1016/j.jmb.2015.08.021.
19. Pan, C., Wu, Q., and Feng, N. (2022). A systematic pan-cancer study demonstrates the oncogenic function of heterogeneous nuclear ribonucleoprotein C. Aging (Albany NY) *14*, 2880–2901. https://doi.org/10.18632/aging.203981.
20. Park, S., Yang, H.D., Seo, J.W., Nam, J.W., and Nam, S.W. (2022). hnRNPC induces isoform shifts in miR-21-5p leading to cancer development. Exp. Mol. Med. *54*, 812–824. https://doi.org/10.1038/s12276-022-00792-2.
21. Xiang, Z., Lv, Q., Zhang, Y., Chen, X., Guo, R., Liu, S., and Peng, X. (2022). Long non-coding RNA DDX11-AS1 promotes the proliferation and migration of glioma cells by combining with HNRNPC. Mol. Ther. Nucleic Acids *28*, 601–612. https://doi.org/10.1016/j.omtn.2022.04.016.
22. Jin, S., Li, M., Chang, H., Wang, R., Zhang, Z., Zhang, J., He, Y., and Ma, H. (2022). The m6A demethylase ALKBH5 promotes tumor progression by inhibiting RIG-I expression and interferon alpha production through the IKKε/TBK1/IRF3 pathway in head and neck squamous cell carcinoma. Mol. Cancer *21*, 97. https://doi.org/10.1186/s12943-022-01572-2.
23. Ma, H., Jin, S., Yang, W., Zhou, G., Zhao, M., Fang, S., Zhang, Z., and Hu, J. (2018). Interferon-alpha enhances the antitumour activity of EGFR-targeted therapies by upregulating RIG-I in head and neck squamous cell carcinoma. Br. J. Cancer *118*, 509–521. https://doi.org/10.1038/bjc.2017.442.
24. Yuan, F., Cai, X., Cong, Z., Wang, Y., Geng, Y., Aili, Y., Du, C., Zhu, J., Yang, J., Tang, C., et al. (2022). Roles of the m(6)A Modification of RNA in the Glioblastoma Microenvironment as Revealed by Single-Cell Analyses. Front. Immunol. *13*, 798583. https://doi.org/10.3389/fimmu.2022.798583.
25. Jiang, L., Zhang, M., Wu, J., Wang, S., Yang, X., Yi, M., Zhang, X., and Fang, X. (2020). Exploring diagnostic m6A regulators in endometriosis. Aging (Albany NY) *12*, 25916–25938. https://doi.org/10.18632/aging.202163.
26. Pan, Z., Zhao, R., Li, B., Qi, Y., Qiu, W., Guo, Q., Zhang, S., Zhao, S., Xu, H., Li, M., et al. (2022). EWSR1-induced circNEIL3 promotes glioma progression and exosome-mediated macrophage immunosuppressive polarization via stabilizing IGF2BP3. Mol. Cancer *21*, 16. https://doi.org/10.1186/s12943-021-01485-6.
27. Ma, Z., Zhou, Y., Wang, Y., Xu, Y., Liu, Y., Liu, Y., Jiang, M., Zhang, X., and Cao, X. (2022). RNA-binding protein hnRNP UL1 binds κB sites to attenuate NF-κB-mediated inflammation. J. Autoimmun. *129*, 102828. https://doi.org/10.1016/j.jaut.2022.102828.
28. Lee, F.F.Y., Harris, C., and Alper, S. (2024). RNA Binding Proteins that Mediate LPS-induced Alternative Splicing of the MyD88 Innate Immune Regulator. J. Mol. Biol. *436*, 168497. https://doi.org/10.1016/j.jmb.2024.168497.
29. Na, Y.R., Stakenborg, M., Seok, S.H., and Matteoli, G. (2019). Macrophages in intestinal inflammation and resolution: a potential therapeutic target in IBD. Nat. Rev. Gastroenterol. Hepatol. *16*, 531–543. https://doi.org/10.1038/s41575-019-0172-4.
30. Cosín-Roger, J., Ortiz-Masiá, D., Calatayud, S., Hernández, C., Esplugues, J.V., and Barrachina, M.D. (2016). The activation of Wnt signaling by a STAT6-dependent macrophage phenotype promotes mucosal repair in murine IBD. Mucosal Immunol. *9*, 986–998. https://doi.org/10.1038/mi.2015.123.
31. Saha, S., Aranda, E., Hayakawa, Y., Bhanja, P., Atay, S., Brodin, N.P., Li, J., Asfaha, S., Liu, L., Tailor, Y., et al. (2016). Macrophage-derived extracellular vesicle-packaged WNTs rescue intestinal stem cells and enhance survival after radiation injury. Nat. Commun. *7*, 13096. https://doi.org/10.1038/ncomms13096.
32. Hegarty, L.M., Jones, G.R., and Bain, C.C. (2023). Macrophages in intestinal homeostasis and inflammatory bowel disease. Nat. Rev. Gastroenterol. Hepatol. *20*, 538–553. https://doi.org/10.1038/s41575-023-00769-0.
33. Jiang, F., Gao, Y., Dong, C., and Xiong, S. (2018). ODC1 inhibits the inflammatory response and ROS-induced apoptosis in macrophages. Biochem. Biophys. Res. Commun. *504*, 734–741. https://doi.org/10.1016/j.bbrc.2018.09.023.
34. Xu, Y., Zhang, Y., Xu, Y., Zang, G., Li, B., Xia, H., and Yuan, W. (2021). Activation of CD137 signaling promotes macrophage apoptosis dependent on p38 MAPK pathway-mediated mitochondrial fission. Int. J. Biochem. Cell Biol. *136*, 106003. https://doi.org/10.1016/j.biocel.2021.106003.
35. Liu, D., Luo, X., Xie, M., Zhang, T., Chen, X., Zhang, B., Sun, M., Wang, Y., Feng, Y., Ji, X., et al. (2022). HNRNPC downregulation inhibits IL-6/STAT3-mediated HCC metastasis by decreasing HIF1A expression. Cancer Sci. *113*, 3347–3361. https://doi.org/10.1111/cas.15494.
36. Deng, X., Qing, Y., Horne, D., Huang, H., and Chen, J. (2023). The roles and implications of RNA m(6)A modification in cancer. Nat. Rev. Clin. Oncol. *20*, 507–526. https://doi.org/10.1038/s41571-023-00774-x.
37. Ma, Y., Zhang, X., Xuan, B., Li, D., Yin, N., Ning, L., Zhou, Y.L., Yan, Y., Tong, T., Zhu, X., et al. (2024). Disruption of CerS6-mediated sphingolipid

metabolism by FTO deficiency aggravates ulcerative colitis. Gut *73*, 268–281. https://doi.org/10.1136/gutjnl-2023-330009.

38. Zhang, T., Ding, C., Chen, H., Zhao, J., Chen, Z., Chen, B., Mao, K., Hao, Y., Roulis, M., Xu, H., et al. (2022). m(6)A mRNA modification maintains colonic epithelial cell homeostasis via NF-κB-mediated antiapoptotic pathway. Sci. Adv. *8*, eabl5723. https://doi.org/10.1126/sciadv.abl5723.
39. Ito-Kureha, T., Leoni, C., Borland, K., Cantini, G., Bataclan, M., Metzger, R.N., Ammann, G., Krug, A.B., Marsico, A., Kaiser, S., et al. (2022). The function of Wtap in N(6)-adenosine methylation of mRNAs controls T cell receptor signaling and survival of T cells. Nat. Immunol. *23*, 1208–1221. https://doi.org/10.1038/s41590-022-01268-1.
40. Zeng, B., Shi, S., Ashworth, G., Dong, C., Liu, J., and Xing, F. (2019). ILC3 function as a double-edged sword in inflammatory bowel diseases. Cell Death Dis. *10*, 315. https://doi.org/10.1038/s41419-019-1540-2.
41. Mortha, A., Chudnovskiy, A., Hashimoto, D., Bogunovic, M., Spencer, S.P., Belkaid, Y., and Merad, M. (2014). Microbiota-dependent crosstalk between macrophages and ILC3 promotes intestinal homeostasis. Science *343*, 1249288. https://doi.org/10.1126/science.1249288.
42. Huang, X.T., Li, J.H., Zhu, X.X., Huang, C.S., Gao, Z.X., Xu, Q.C., Zhao, W., and Yin, X.Y. (2021). HNRNPC impedes m(6)A-dependent anti-metastatic alternative splicing events in pancreatic ductal adenocarcinoma. Cancer Lett. *518*, 196–206. https://doi.org/10.1016/j.canlet.2021.07.016.
43. Crocker, P.R., Paulson, J.C., and Varki, A. (2007). Siglecs and their roles in the immune system. Nat. Rev. Immunol. *7*, 255–266. https://doi.org/10.1038/nri2056.
44. Kaemmerer, E., Kuhn, P., Schneider, U., Clahsen, T., Jeon, M.K., Klaus, C., Andruszkow, J., Härer, M., Ernst, S., Schippers, A., et al. (2015). Beta-7 integrin controls enterocyte migration in the small intestine. World J. Gastroenterol. *21*, 1759–1764. https://doi.org/10.3748/wjg.v21.i6.1759.
45. Yang, Y., Hsu, P.J., Chen, Y.S., and Yang, Y.G. (2018). Dynamic transcriptomic m(6)A decoration: writers, erasers, readers and functions in RNA metabolism. Cell Res. *28*, 616–624. https://doi.org/10.1038/s41422-018-0040-8.
46. Yang, L., Wu, G., Wu, Q., Peng, L., and Yuan, L. (2022). METTL3 overexpression aggravates LPS-induced cellular inflammation in mouse intestinal epithelial cells and DSS-induced IBD in mice. Cell Death Dis. *8*, 62. https://doi.org/10.1038/s41420-022-00849-1.
47. Singh, V., Gowda, C.P., Singh, V., Ganapathy, A.S., Karamchandani, D.M., Eshelman, M.A., Yochum, G.S., Nighot, P., and Spiegelman, V.S. (2020). The mRNA-binding protein IGF2BP1 maintains intestinal barrier function by up-regulating occludin expression. J. Biol. Chem. *295*, 8602–8612. https://doi.org/10.1074/jbc.AC120.013646.
48. Xie, J., Li, Q., Zhu, X.H., Gao, Y., and Zhao, W.H. (2019). IGF2BP1 promotes LPS-induced NFκB activation and pro-inflammatory cytokines production in human macrophages and monocytes. Biochem. Biophys. Res. Commun. *513*, 820–826. https://doi.org/10.1016/j.bbrc.2019.03.206.
49. Haber, A.L., Biton, M., Rogel, N., Herbst, R.H., Shekhar, K., Smillie, C., Burgin, G., Delorey, T.M., Howitt, M.R., Katz, Y., et al. (2017). A single-cell survey of the small intestinal epithelium. Nature *551*, 333–339. https://doi.org/10.1038/nature24489.
50. Ke, Z., Huang, Y., Xu, J., Liu, Y., Zhang, Y., Wang, Y., Zhang, Y., and Liu, Y. (2024). Escherichia coli NF73-1 disrupts the gut-vascular barrier and aggravates high-fat diet-induced fatty liver disease via inhibiting Wnt/β-catenin signalling pathway. Liver Int. *44*, 776–790. https://doi.org/10.1111/liv.15823.
51. Liu, Y., Xu, J., Ren, X., Zhang, Y., Ke, Z., Zhou, J., Wang, Y., Zhang, Y., and Liu, Y. (2022). Cholecystectomy-induced secondary bile acids accumulation ameliorates colitis through inhibiting monocyte/macrophage recruitment. Gut Microb. *14*, 2107387. https://doi.org/10.1080/19490976.2022.2107387.

STAR★METHODS

KEY RESOURCES TABLE

REAGENT or RESOURCE	SOURCE	IDENTIFIER
Antibodies		
Rabbit monoclonal anti- HNRNPC	Zen-bio	Cat# R381235; RRID: AB_ 3099728
Rabbit polyclonal anti- HNRNPC	Proteintech	Cat# 11760-1-AP; RRID: AB_2117500
Mouse monoclonal anti-GAPDH	Proteintech	Cat# 10494-1-AP; RRID: AB_2263076
Mouse monoclonal anti-GAPDH	Abcam	Cat# ab8245; RRID: AB_2107448
TruStain FcX(TM) anti-mouse CD16/32	Biolegend	Cat# 101319; RRID:AB_1574975
FITC anti-mouse CD3	Biolegend	Cat# 100203; RRID: AB_312660
FITC anti-mouse CD14	Biolegend	Cat# 123307; RRID: AB_940578
FITC anti-mouse CD19	Biolegend	Cat# 152403; RRID: AB_2629812
FITC anti-mouse CD34	Thermo Scientific	Cat# 11-0341-82; RRID: AB_465021
FITC anti-mouse TCRβ	Biolegend	Cat# 109206; RRID: AB_313429
FITC anti-mouse TCR γ	Biolegend	Cat# 118105; RRID: AB_313830
FITC anti-mouse CD11b	Biolegend	Cat# 101205; RRID: AB_312788
FITC anti-mouse CD11c	Biolegend	Cat# 117305; RRID: AB_313775
FITC anti-mouse Gr-1	Biolegend	Cat# 108405; RRID: AB_313370
FITC anti-mouse TER-119	Biolegend	Cat# 116206; RRID: AB_313707
FITC anti-mouse FcERI α	Biolegend	Cat# 134305; RRID: AB_1626102
FITC anti-mouse CD45	Biolegend	Cat# 157213; RRID: AB_2894427
PE anti-mouse CD3	Biolegend	Cat# 100205; RRID: AB_312662
APC anti-mouse CD4	Biolegend	Cat# 116013; RRID: AB_2563024
PE/Cyanine7 anti-mouse CD8a	Biolegend	Cat# 100721; RRID: AB_312760
APC/Cyanine7 anti-mouse/human CD45R/B220	Biolegend	Cat# 103223; RRID: AB_313006
PE/Cyanine7 anti-mouse F4/80	Biolegend	Cat#123113; RRID: AB_893490
PE anti-mouse/human CD11b	Biolegend	Cat# 101207; RRID: AB_312790
PE/Dazzle^{TM} 594 anti-mouse CD86	Biolegend	Cat#105042; RRID: AB_2566409
APC anti-mouse CD206 (MMR)	Biolegend	Cat#141707; RRID: AB_10896057
APC anti-mouse CD45	Biolegend	Cat# 103112; RRID: AB_312977
Brilliant Violet 650 anti-mouse CD127	Biolegend	Cat#135043; RRID: AB_2629681
Brilliant Violet 785 anti-mouse KLRG1	Biolegend	Cat# 138429; RRID: AB_2629749
Brilliant Violet 510^{TM} anti-mouse CD335 (NKp46)	Biolegend	Cat# 137623; RRID: AB_2563290
PE anti-mouse ROR gamma (t)	eBioscience	Cat# 12-6988-82; RRID: AB_1834470
Goat Anti-Rabbit IgG H&L (Alexa Fluor 405) secondary antibody	Zen-bio	Cat#550106
HRP-conjugated secondary antibody (anti-rabbit)	ZSGB-Bio	Cat#ZB-2301
HRP-conjugated secondary antibody (anti-mouse)	ZSGB-Bio	Cat# ZB-2305
Chemicals, peptides, and recombinant proteins		
Dextran Sulfate Sodium Salt	MP Biomedicals	Cat# 0216011090
TRIzol	Invitrogen	Cat # 15596026
POWRUP SYBR MASTER MIX	Invitrogen	Cat#A25742
RIPA lysis buffer	Applygen Technologies	Cat#C1053
protease and phosphatase inhibitor cocktails	Thermo Scientific	Cat#78440
phosphate-buffered saline	Gibco	Cat# C10010500BT
(RPMI) 1640	Gibco	Cat# C11875500BT
0.5M EDTA	Solarbio	Cat# E1170
4-(2-hydroxyethyl) piperazine-1-ethanesulfonic acid (HEPES)	Thermo Scientific	Cat# H8090

(*Continued on next page*)

Continued

REAGENT or RESOURCE	SOURCE	IDENTIFIER
dithiothreitol	Sigma Aldrich	Cat# 3483-12-3
fetal bovine serum	Sigma Aldrich	Cat# F8687
Phorbol 12-Myristate 13-Acetate(PMA)	MultiSciences Biotech	Cat# CS0001
2-Mercaptoethanol	Gibco	Cat# 2603108
Percoll	Cytiva	Cat# 10338148
Dulbecco's Modified Eagle medium (DMEM)	Gibco	Cat# C11995500BT
Penicillin-Streptomycin	Invitrogen	Cat# 15140122
lipopolysaccharide	Sigma Aldrich	Cat# L2630
DNase I	Sigma Aldrich	Cat#10104159001
collagenase IV	Sigma Aldrich	Cat# C4-22
fixation buffer	Biolegend	Cat#420801
permeabilization wash buffer	Biolegend	Cat#421002
Mycoplasma Elimination Reagent	Yeasen	Cat#40607ES03
Actinomycin D	Bioss	Cat#D50409s
Critical commercial assays		
BCA protein assay kit	Thermo Scientific	Cat#23227
Reveraid First Strand cDNA Synthesis Kit	Thermo Scientific	Cat# K1622
CALNP^{TM} RNAi *in vitro*	D-nano	Cat# N001-01
Deposited data		
Raw Single-cell sequencing data	https://ngdc.cncb.ac.cn/gsa.	HRA005538
Raw RNA-seq data	https://ngdc.cncb.ac.cn/gsa/	CRA017763
Experimental models: Cell lines		
Raw264.7 cells	Procell	N/A
Oligonucleotides		
qPCR primers, see Table S1 and S2.	This paper	N/A
siRNA targeting sequence(mice): HNRNPC #1: CCUUUGUCCAGUAUGUUAATT; HNRNPC#2: CUUUCAACGGGAUUAUUAUTT; HNRNPC#3: GGAUGAUG ACGAUAAUGAATT	This paper	N/A
siRNA targeting sequence(human H3183): HNRNPC: Sense: CAACGGGACUAUUAUGAUA Antisense: UAUCAUAAUAGUCCCGUUG	This paper	N/A
Software and algorithms		
FlowJo 10.8.1	Treestar	https://www.flowjo.com/solutions/flowjo
ImageJ software	NIH	https://imagej.nih.gov/ij/
GraphPad Prism 9	GraphPadSoftware	https://www.graphpad.com/
Single R software	Haber et al.,2017[49]	https://github.com/dviraran/SingleR
Cluster Profiler R package	Ke et al.,2024[50]	http://www.R-project.org/

EXPERIMENTAL MODEL AND STUDY PARTICIPANT DETAILS

Ethics approval and experimental animals

Male C57BL/6 J wild-type mice aged 6–8 weeks were purchased from Beijing Vital River Laboratory Animal Technology Co. Ltd (Beijing, China). All animal experiments were reviewed and approved by the Institutional Medical Ethics Review Board of Peking University People's Hospital (ethical approval number: 2021PHE023). The mice were housed under specific pathogen–free conditions with a 12 h-light/dark cycle and they could acclimate for one week with free access to water and food before the experiments. The SPF rooms comply with the Chinese national standard for Experimental Animal Environment and Facilities (GB14925-2010), maintaining a housing temperature between 20°C and 26°C and a relative humidity of 40–70%.The specific treatment procedures for the mouse model are outlined in the method details section.

METHOD DETAILS

Induction of acute dextran sulfate sodium colitis mouse model

Acute C57BL/6 J murine colitis models were induced with 2.5% DSS (Dextran Sulfate Sodium Salt, MP Biomedicals) in drinking water for 7 days and then with regular drinking water for another 3 days. The weight and stool conditions of mice were observed at the same time point every day throughout experimental colitis. The mice were euthanized on day 10 and then the colon length was measured immediately; distal colonic tissue and feces were harvested for further study and the remaining colon tissue was used for subsequent flow cytometry analysis.

Hematoxylin and eosin (H&E) staining

Colon tissue was cut into 0.5 cm pieces. The pieces were then fixed in 4% paraformaldehyde, embedded in paraffin, and cut into 4-μm-thick sections. The sections were stained with standard hematoxylin and eosin (H&E) staining. Histological evaluation was performed by two blinded investigators. The sections were observed and images were captured using a ZEISS microscope (Germany). Images were viewed and captured using a ZEISS microscope (Germany).

RNA extraction and quantitative real-time PCR (qPCR)

Total RNA of cultured cells was extracted using TRIzol reagent (Invitrogen). For colon tissues, total RNA was extracted with total RNA kit (Omegabiotek). The reverse transcriptase kit (Thermo Scientific) was used to synthesize complementary DNA (cDNA). The POWRUP SYBR MASTER MIX (Applied Biosystems) was employed for quantitative real-time PCR and qPCR was conducted on the Applied Biosystems StepOne Plus Real-Time PCR System with SYBR Green Master Mix (Thermo Fisher Scientific). GAPDH mRNA level was used as an internal control to calculate mRNA relative abundance. The primer sequences used for qPCR in mice and human were displayed in Tables S1 and S2.

Western blot

Total protein of colonic tissue and macrophages were lysed in radioimmunoprecipitation assay (RIPA) lysis buffer supplemented with protease and phosphatase inhibitor cocktails on ice for 30 min. The lysis was then centrifuged for 20 min for the acquirement of protein supernatant. And protein concentrations were quantified with PierceTM BCA protein assay kit. Antibodies against HNRNPC (1:2000, Zen-bio used for Western blot of Raw264.7 cells and THP-1 cells; 1:10000, Proteintech, used for Western Blot of colonic tissues), and glyceraldehyde-3-phosphate dehydrogenase (GAPDH) (1:10000, Proteintech, used for Western blot of Raw264.7 cells; 1:1000 Abcam, used for Western blot of THP-1 cells) were used in TBST (TBS with 1% Tween) at 4°C overnight. After washing the membrane with TBST three times, an HRP-conjugated secondary antibody (ZSGB-Bio, China, anti-rabbit: ZB-2301; anti-mouse: ZB-2305; both at dilutions of 1:3000) was incubated at room temperature for 1 h. The membrane was washed again three times, and the signals were detected with enhanced chemiluminescence (ECL) with pico ECL and visualized using Amersham Imager 600 System (GE Healthcare Bio-Sciences) and quantified by using ImageJ software (National Institutes of Health, USA).

Isolation of colon lymphocytes from the lamina propria

Isolation of colon lymphocytes from the lamina propria is as described.[51] In brief, mouse colon tissues were harvested and feces and fatty tissues were discarded. Then, the colon tissues were cut apart longitudinally, washed in precooled phosphate-buffered saline (PBS) four times, and incubated in Roswell Park Memorial Institute (RPMI) 1640 (containing 5 mM EDTA, 20 mM 4-(2-hydroxyethyl) piperazine-1-ethanesulfonic acid (HEPES), 1 mM dithiothreitol, and 5% (vol/vol) fetal bovine serum) for 30 min at 37°C. Digested remaining liquid was collected for the harvest of colon epithelial cells. Next, colon tissues were washed in PBS four times, cut into minimal pieces, and subsequently incubated in digestion buffer (0.2 mg/mL collagenase IV (Sigma Aldrich), 0.2 mg/mL DNase I (Sigma-Aldrich), 5% (vol/vol) FBS) for 30 min at 37°C. All remaining digested tissues were filtered through a 70-μm strainer, and the filtrates were collected and centrifuged at 700 g for 7 min. The supernatant was discarded and the precipitates were resuspended with 30% Percoll gradient centrifugation and centrifuged at 2000 g for 20 min for the purification of lymphocytes.

Isolation of colon epithelial cells

Following the methods described by previous researchers,[38] we isolated intestinal epithelial cells. In brief, after pre-digesting the colon tissue for 30 min as described above, the remaining pre-digestion solution was transferred to a 15mL centrifuge tube, and were subsequently filtered through a 70-μm strainer. The filtrate was collected and then centrifuged at 1000r for 5 min. Next, the supernatant was discarded and the remaining precipitates were mostly epithelial cells.

Flow cytometry analysis

As described above, the purified lymphocytes were harvested and washed in staining buffer (PBS containing 2% FBS) three times. Cell suspensions were incubated with anti-mouse CD16/32 antibody for 10 min to block Fc receptors. Cells were then stained with surface antibodies for 30 min at 4°C. For intracellular staining, cells were fixed in fixation buffer, permeabilized in intracellular staining permeabilization wash buffer, and stained with intracellular antibodies for 30 min at room temperature. For intracellular HNRNPC staining, cells were incubated with hnRNP C1/C2 Rabbit mAb (Zen-bio) followed by Goat Anti-Rabbit IgG H&L (Alexa Fluor 405)

secondary antibody (Zen-bio). For assessing ILCs, lineage markers include CD3 (17A2), CD14(Sa14-2), CD19 (1D3/CD19), CD34 (HM34), TCRα(H57-597), TCR γ(UC7-13D5), CD11b (M1/70), CD11c (N418), FcERI α(MAR-1), TER-119 (TER-119) and Gr-1 (RB6-8C5), which are labeled with FITC. Anti-mouse antibodies FITC-CD45(S18009F), PE-CD3(17A2), APC-CD4(GK1.5), PE/Cyanine7-CD8a(S18018E), APC/Cyanine7-B220(RA3-6B2), PE/Cyanine7-F4/80(BM8), PE-CD11b(M1/70), CF594-CD86(GL-1), APC-CD206(GL-1), FITC- lineage, APC-CD45(I3/2.3), Brilliant Violet 650-CD127(A7R34), Brilliant Violet 785-KLRG1(2F1/KLRG1), Brilliant Violet 510-Nkp46(29A1.4) were purchased from BioLegend; anti-mouse antibodies PE-RORγt (AFKJS-9) were purchased from eBioscience. Data was acquired on the LSRFortessa (BD) and analyzed by FlowJo10.8.1 software.

Cell culture

Raw264.7 cells were cultured in a humidified incubator at 37°C with 5% CO2 in Dulbecco's Modified Eagle medium containing 10% fetal bovine serum, 100 μL/mL of penicillin, and 100 μL/mL of streptomycin. For induction of inflammatory condition, Raw264.7 cells are stimulated with 1 μg/mL lipopolysaccharide for 2h, 4h, 6h, 12h and 24h respectively. Cells and supernatants were then collected for subsequent experiments.

THP-1 cells were cultured in a humidified incubator at 37°C with 5% CO2 in RPMI 1640 medium containing 10% fetal bovine serum, 1% penicillin–streptomycin, 0.1% β – mercaptoethanol. For differentiation into macrophages, cells were incubated with 100 ng/mL Phorbol 12-myristate 13-acetate (PMA) for 48 h. For induction of inflammatory condition, THP-1 cells are stimulated with 100 ng/mL and 500 ng/ml lipopolysaccharide for 4h or 24h respectively.

All the cell lines used in this study have been authenticated. And we employed routinely mycoplasma elimination reagent to prevent mycoplasma contamination.

siRNA knockdown

CALNP RNAi *in vitro* (D-nano, China) was used to transfect small interfering RNA (siRNA) (20nM) into Raw264.7 cells according to the manufacturer's instructions strictly. Briefly, when the Raw264.7 cells were in good condition, we seeded 100,000 cells into every well of a 24-well plate. After 12 h, we replaced the culture medium with fresh medium and added a pre-prepared mixture of siRNA and transfection reagents. We gently mixed the contents and proceeded to culture the cells. During the subsequent first 24 h, we did not replace the medium. 24 h after transfection, mRNA expression of HNRNPC was measured; 48 h after transfection, protein level was detected. The siRNA sequences targeting HNRNPC were designed and synthesized by TsingKe Biological Technology (Beijing, China) and sequences are listed in the key resources table.

For siRNA's transfection into THP-1 cells, we still employed the transfection reagent CALNP RNAi *in vitro* (D-nano, China). We seeded 100,000 cells into every well of a 24-well plate added with PMA. After 48 h, we replaced the culture medium with fresh medium and added a pre-prepared mixture of siRNA and transfection reagents. 24 h after transfection, mRNA expression of HNRNPC was measured; 48 h after transfection, protein level was detected.

Adoptive transfer of Raw264.7 cells into mice with DSS-induced colitis

Raw264.7 cells were transfected siRNA targeting HNRNPC and negative control siRNA as mentioned above. After validation of knockdown efficiency of HNRNPC in the Raw264.7 cells (Raw264.7 cells transfected with siRNA targeting HNRNPC were called Raw-siHNRNPC; Raw264.7 cells transfected with negative control siRNA were called Raw-siNC), Raw-siHNRNPC cells and Raw-siNC cells were respectively injected intravenously into C57BL/6 J wild-type mice. C57BL/6 J Mice were randomly divided into two groups, i.e., DSS+Raw-siNC and DSS+ Raw-siHNRNPC group. Mice in DSS+Raw-siNC and DSS+ Raw-siHNRNPC groups were respectively given 2×10^6 cells (in 200 μL of PBS) by tail vein injection on day 0, 3, 5, and 7 of DSS-induced colitis. And details of induction of acute colitis are as mentioned above.

Single-cell RNA sequencing (scRNA-Seq) and bioinformatic analysis

We made the bioinformatic analysis with single-cell sequencing data published before from our research group (The single-cell RNA sequencing data has uploaded to the public database https://ngdc.cncb.ac.cn/gsa. and the number is HRA005538). Briefly, we collected colonic mucosa endoscopically from healthy controls and patients with UC. And samples from UC patients were got from inflamed areas. And this study has been approved by the Institutional Medical Ethics Review Board of Peking University People's Hospital (ethical approval number: 2019PHB125-01 and 2019PHB126-01). Single cells were isolated using the 10X Genomics' Chromium single-cell sequencing technology, followed by amplification of complementary DNA and library construction. The scRNA-seq library was generated using the Chromium Single Cell 3' Library & Gel Bead Kit v.2 (PN-120237, 10× Genomics). The cDNA and library concentrations were assessed using the HS dsDNA Qubit Kit according to the manufacturer's instructions. The sample pools were adjusted to a final concentration of 7.5 nM, and the library pool concentration was quantified using the Library Quantification qPCR Kit from KAPA Biosystems. The libraries marked with barcodes were sequenced using the Illumina NovaSeq 6000. Cell Ranger v6.1.1 demultiplexed FASTQ reads, aligned to hg38 transcriptome, and extracted ''cell'' and ''UMI'' barcodes, generating DGE matrix recording gene-specific UMIs for each cell barcode. Then, we utilized Seurat v4.3.1 to perform cell filtration, normalization, clustering, gene expression analysis, and identification of marker genes. Low-quality cells with fewer than 500 genes and more than 25% mitochondrial genes were removed. After filtering the data, we normalized it using the ''LogNormalize'' parameter. We then clustered single cells into distinct colonic cell subsets according to a previous study by Haber et al.[49] And for cell type

annotation, the SingleR software along with ''HumanPrimaryCellAtlasData'' and ''DatabaseImmuneCellExpressionData'' databases were used. After clustering the various colonic cells, we conducted an analysis of the expression of different m6A regulators within these cell types.

Bulk RNA sequencing (RNA-Seq) and bioinformatic analysis

Total RNA from Raw264.7 cells was extracted using Trizol reagent (Invitrogen). Agilent 5400 was employed to test RNA quality. In-house R scripts were used to process the Raw data in *fastq* format. *HTSeq* v0.11.2 was used to count the reads numbers mapped to each gene. Differential expression analysis between Raw264.7 cells with and without HNRNPC knockdown was performed using the *DESeq2* R package. Based on the method we previously employed,[50] the *clusterProfiler* R package was used to perform Gene Ontology (GO) enrichment analysis on differentially expressed genes, with correction for gene length bias. Pathways with an adjusted *p*-value of less than 0.05 were regarded as significantly enriched. The *clusterProfiler* package was used to conduct Gene Set Enrichment Analysis (GSEA) to identify upregulated and downregulated pathways; pathways with absolute values of normalized enrichment score (NES) greater than 1 and a *p*-value below 0.05 were chosen for further analysis. (The RNA-sequencing data has uploaded to the public database https://ngdc.cncb.ac.cn/gsa. and the number is CRA017763).

RNA stability assay

To evaluate mRNA stability, we used actinomycin D to inhibit generation of new mRNA and detected mRNA level of possible target genes. Briefly, 24 h after treating cells with siRNA, we replaced fresh cell culture medium and added actinomycin D to cells (The final concentration of actinomycin D is 2ug/ml[35]). Cells were collected at 1, 2, and 4 h following the addition of actinomycin D. Subsequently, total RNA of cells was extracted and cDNA was synthesized. qPCR was conducted for the detection of the relative mRNA levels of target genes at different time points.

QUANTIFICATION AND STATISTICAL ANALYSIS

Data was presented as a mean value ±SEM of triplicate experiments. Statistical analysis was measured by the parametric (Student's *t* test) test to compare the values between the two groups. One-way ANOVA was applied to analyze the differences of data of more than two groups. All graphs and statistical analysis were performed by GraphPad Prism 9. A p value < 0.05 was considered statistically significant with significance levels indicated as follows: $^{*}p < 0.05$, $^{**}p < 0.01$, $^{***}p < 0.001$, $^{****}p < 0.0001$, and ns for not significant. *p* values are indicated in each figure legend. N represents number of animals and cell duplicates. And all the statistical details of experiments can be found in the figure legends and figures.